

EFFECT OF AGGRESSIVE ENVIRONMENTS ON MECHANICAL PERFORMANCE OF FIBRE CERAMIC COMPOSITES



Award No. FA 4869 – 06 -1 -0046

**Asian Office of Aerospace Research & Development (AOARD)
7-23-17, Roppongi, Minato-Ku, Tokyo, 160-0032, JAPAN**



**Prof. V. K. SRIVASTAVA
Co-ordinator
Department of Mechanical Engineering
Institute of Technology
Banaras Hindu University
VARANASI – 221005, INDIA**

July 2007

Report Documentation Page

*Form Approved
OMB No. 0704-0188*

Public reporting burden for the collection of information is estimated to average 1 hour per response, including the time for reviewing instructions, searching existing data sources, gathering and maintaining the data needed, and completing and reviewing the collection of information. Send comments regarding this burden estimate or any other aspect of this collection of information, including suggestions for reducing this burden, to Washington Headquarters Services, Directorate for Information Operations and Reports, 1215 Jefferson Davis Highway, Suite 1204, Arlington VA 22202-4302. Respondents should be aware that notwithstanding any other provision of law, no person shall be subject to a penalty for failing to comply with a collection of information if it does not display a currently valid OMB control number.

1. REPORT DATE 21 AUG 2007	2. REPORT TYPE FInal	3. DATES COVERED 26-04-2006 to 06-08-2007	
4. TITLE AND SUBTITLE Effect of Aggressive Environment on Mechanical Performance of Fiber Ceramic Composites		5a. CONTRACT NUMBER FA48690610046	
		5b. GRANT NUMBER	
		5c. PROGRAM ELEMENT NUMBER	
6. AUTHOR(S) Vijay Srivastava		5d. PROJECT NUMBER	
		5e. TASK NUMBER	
		5f. WORK UNIT NUMBER	
7. PERFORMING ORGANIZATION NAME(S) AND ADDRESS(ES) Banaras Hindu University, Institute of Technology, BHU, Institute of Technology, Varanasi., Varanasi 221005 India, IN, 221005		8. PERFORMING ORGANIZATION REPORT NUMBER N/A	
9. SPONSORING/MONITORING AGENCY NAME(S) AND ADDRESS(ES) AOARD, UNIT 45002, APO, AP, 96337-5002		10. SPONSOR/MONITOR'S ACRONYM(S) AOARD	
		11. SPONSOR/MONITOR'S REPORT NUMBER(S) AOARD-064042	
12. DISTRIBUTION/AVAILABILITY STATEMENT Approved for public release; distribution unlimited			
13. SUPPLEMENTARY NOTES			
14. ABSTRACT Based on the experimental observation, the results clearly indicate that weight of C/C-SiC composite is damaged severally at about 2% and 2D C/C composite damaged nearly 12%, when oxidised in open atmosphere by the flame of oxy-acetylene gas. The changes in microhardness, XRD pattern and thermal properties are appeared because of delamination, debonding, pyrolysis of matrix and formation of CO, CO2 and SiO2. Therefore, maximum tensile and compressive stress of ceramic composites decreased with the oxidation time in open atmosphere by oxyacetylene gas flame. Also, SiC ceramic coating on 4D carbon composites resulted that the carbon?carbon composite temperature predicts the oxidation kinetic is severe after 1273K. This was due to formation of smooth silicon carbide film phases covering the surface of the composite. Which is less volatile and showed lower oxygen permeability, and consequently acted as an effective oxygen diffusion barrier? The whole study show that a combination of both silicon and carbon based materials system is more useful for elevated oxidation protection of carbon-carbon composites.			
15. SUBJECT TERMS Ceramic Matrix Composites, Carbon-Carbon composites, C/C composites, C/C composites, microstructure, properties, joining			
16. SECURITY CLASSIFICATION OF:			17. LIMITATION OF ABSTRACT Same as Report (SAR)
a. REPORT unclassified	b. ABSTRACT unclassified	c. THIS PAGE unclassified	
			18. NUMBER OF PAGES 36
			19a. NAME OF RESPONSIBLE PERSON

Acknowledgements

I have great pleasure in expressing my deep sense of gratitude and indebtedness to Dr. J. P. Singh, Programme Manager, AOARD-AFOSR, Tokyo, Japan for his most valuable support and active advice of this research project. Also, it gives immense pleasure to gratefully acknowledge Dr. Ken C. Goretta, Programme Director, AOARD-AFOSR, Tokyo, Japan for the implementation of this international project on “Effects of Aggressive Environments on Fibre Composites”. Thanks are gratefully extended to office staff of AOARD, Tokyo, Japan for their full co-operation.

I must express my sincere appreciation to my entire laboratory staff and BHU administration for their assistance during the course of this project.

(Co-ordinator)
Dr. V.K. Srivastava
Professor
Dept. of Mechanical Engineering
Institute of Technology, BHU
Varanasi – 221005, INDIA

LIST OF CONTENTS

	Acknowledgements	i
	Details of expenditure	ii
1.	Introduction	1
1.1.	Carbon-carbon composite	1
1.2.	Carbon-carbon-silicon-carbide composites	3
1.3.	Comparative chart	7
2.	Experimental procedure	8
2.1.	Materials preparation & tests	8
2.1.1.	C/C composites	8
2.1.2.	C/C-SiC composites	8
2.2.	Effect of oxidations	10
2.2.1.	Exposure with gas flame on C/C-SiC composites	10
2.2.1.1	Microharness test	12
2.2.1.2.	XRD & thermal analysis	13
2.2.2.	Exposure of temperature on C/C composites	15
2.2.2.1.	Oxidation performance of SiC coated C/C composite	18
2.2.3.	Mechanical performance of composites	20
2.2.3.1.	Tensile & compressive tests	20
2.2.3.2.	SEM test	25
3.	Discussions	26
3.1.	Effects of oxidation on composites	26
3.2.	Micro-performance of composites	28
4.	Conclusions	29
5.	References	30
6.	Publications	32
7.	Work schedule for 2 nd year	32
8.	Grant required for 2 nd year	32

Details of Expenditure:

i. Sanctioned Amount:

\$ 23160.0
(Rs. 10.82 Lakh)

ii. Expenditure:

S. No.	Items	Price, Rs.
1.	Automated Universal Testing Machine,	2,68,275.0
2.	Pentium x 4 Computer with Laser Printer	44690.0
3.	Electronic Balance	4500.0
4.	Soldering kits	6525.0
5.	Advertisement	1,15,245.0
6.	Salary and travel	2,85,000.0
7.	Contingency, materials and stationary, postage etc.	3,58,000.0
	Total	10,82,235.00

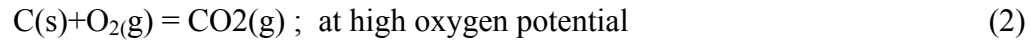
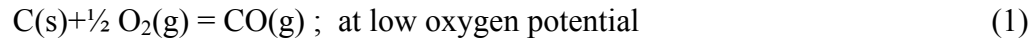
1. INTRODUCTION:

1.1. Carbon-Carbon Composites

Carbon-carbon (C/C) composite materials have been developed in the 1960s to satisfy the needs of high temperature applications in different high-tech industries, especially in aerospace and aeronautics such as the combustion chamber of ballistic missiles, re-entry vehicles, aircraft, brake discs, etc. C/C composites have many of the desirable high-temperature properties of conventional carbons, including excellent mechanical properties. In addition, low density, very low coefficient of expansion, excellent thermal conductivity, high heat absorption capacity, and stable coefficient of dynamic friction and, finally, a reasonable wear rate produce an unprecedented material for brake applications. In many of these applications the load is applied dynamically, resulting in the development of high rates of strain and stress. The ability to predict failure of these structures under dynamic loading is becoming increasingly important. In dynamic conditions, disturbances in the form of stress waves emanate from the point of impact and propagate through the structure. Propagation of these waves through C/C composites will be significantly different from what is usually found with homogeneous materials. Because of the complexity introduced by the inertia forces, such as variation in the properties with the rate of loading, damage initiation and growth during the loading process, the principles of dynamic elasticity have not been well understood. To study the complex phenomena associated with the stress waves, a clear distinction must be made between the material response and the structural response. On this latter point it is noted that the response of a structure depends on its geometry, the point of application of the load, and the way in which the material comprising the structure responds.

Carbon is often used as a construction material for high temperature, non-oxidizing systems. Modern carbon materials such as continuous fiber reinforced carbon composites (CFRCC) are being developed for commercial as well as aerospace applications [1]. This include heat shields, aircraft as well as other brake systems, vacuum furnace parts, heat exchangers, lining for chemical reactors and a host of other industrial applications [2].The performance of these thermo-structural composites is drastically reduced due to rapid oxidation of carbon at elevated temperature. The uncoated CFRCC loses its weight and shape with increase in exposed high

temperature environment. Gasification of carbon typically begins at 623K with following gas-solid reactions.



Thermodynamically, unless the oxygen pressure is extremely low (i.e., $< \sim 10^{-10}$ atm), some carbon will always be lost via these reactions. For long term application at such conditions it is essential that these composites should be protected against oxidation. For this purpose, SiC ceramics are primarily preferred as the coating material. This is due to their good compatibility with C/C composites, having reasonable strength, high thermal conductivity, excellent corrosion and oxidation resistance [3]. However the expected life of SiC coating is limited by its oxidation properties. At temperatures above 973K in air, Si-C reacts with air to form CO and a silica-rich surface layer. With change in operating condition, the most obvious chemical issues are generation of silicon sub oxides and simple vaporization of the oxides at high temperatures. The vapour species above SiO₂(s) consist of a mixture of SiO(g), SiO₂(g), and other species depending on conditions. At low pressure oxygen environment, SiO₂ decomposes to an oxygen product such as:



Vaporization leads to material loss, possible roughening of the surface, and deposition of the crystal composition on colder parts of the system. Often at 'carbon and SiC' interface SiO₂ is also formed. C/SiO₂ solid phases are not compatible and generate some small amounts of volatile species within 1000-2000K. Since highly viscous SiO₂ is not able to bridge the 'crazing and debonding' of SiC coating, it induces the degradation of SiC coating. For having active crack bridging therefore, other oxides are necessary.

Thus to have a satisfactory performance of carbon- carbon composites, development of a suitable functionally gradient anti-oxidation coating is the logical choice [4]. Among all carbon composites, four directional reinforced composite represents a less studied C/C material system. Selective materials such as MoSi₂ and B₄C have promising oxidation resistance at high temperatures. MoSi₂ has a high melting point with excellent high-temperature characteristics and high resistance against oxidation. There is a good thermodynamic compatibility between SiC and MoSi₂ [5]. MoSi₂ exhibits a brittle-to-ductile transition in the vicinity of 1173K–1273K and

above this temperature shows significant metal-like ductility [6-7]. Therefore it is expected that MoSi_2 can improve the high temperature functional properties of SiC material and thus has a Fan and Song et al. have studied fine-grained SiC- B_4C doped graphite prepared by the ball milling dispersion method [8]. It possesses excellent self-healing properties and oxidation resistance at 1673K. Kobayashi and Miyazaki et al. found that mixing some kinds of ceramic powders (B_4C -SiC) into the carbon substrates could produce carbon-ceramic composites with high oxidation resistance and self-healing properties capable of resisting oxidation at high temperatures [9].

1.2. Carbon-Carbon-Silicon Carbide Composites

To make full use of carbon-carbon composites in high-temperature applications and also in oxidising atmospheres, additional oxidation protection is required. Oxidation behaviour of carbon and of carbon-carbon composites have been studied over the past two decades [10-14] with a view on practical applications of these materials at varying temperatures under different environmental conditions. This area is still in focus from the point of view of basic scientific interest, especially when new methods of carbon matrix modification, processing and oxidation protection for carbon-carbon composites are being explored. Carbon matrix obtained from different precursors possesses different types of texture and microstructure on which the oxidation rate largely depends. Silicon based oxidation inhibitors are most popular for oxidation protection of carbon-carbon composites. They are often added to the matrix either as carbides or as oxides which then are converted into carbides. An important siliconising process for carbon-carbon composites is the liquid silicon infiltration (LSI) method to form carbon-carbon silicon carbide composites (C/C-SiC). This process consists of three major steps. First, a carbon fibre reinforced plastic is produced. Second, the green composite is pyrolysed and the shrinkage of the polymeric matrix is hindered by the fibres which lead to the development of a regular crack pattern. In the last step, the carbon-carbon preform is infiltrated with liquid silicon that reacts to SiC, yielding a dense material with carbon-carbon segments separated from each other by SiC. The LSI method leads to a damage tolerant ceramic material that has a significantly lower component fabrication time and therefore reduced component costs compared with other ceramic

matrix composite (CMC) manufacturing processes [15]. Carbon fibres are the back bone of C/C and C/C–SiC composites.

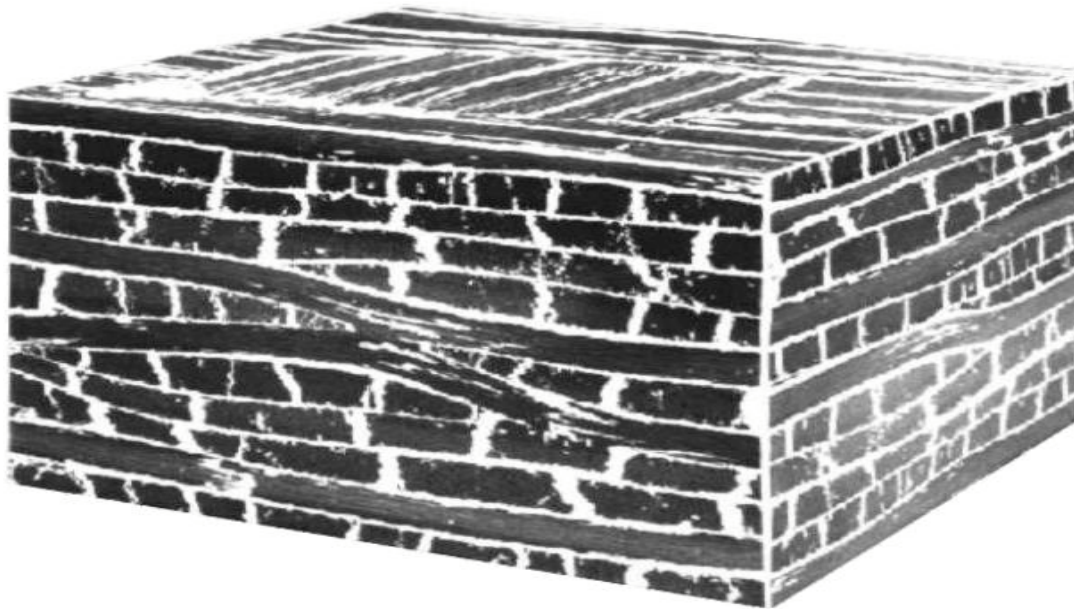


Fig. 1. 3D of C/C-SiC Composites

The latest advancement in C/C composites is largely attributed to the improvement in carbon fibre properties such as stiffness, modulus of elasticity, fatigue strength, and lower thermal expansion coefficient. High strength and high modulus carbon fibres are about 7–8 μm in diameter and consist of small crystallites of graphite. In graphite single crystal carbon atoms are arranged in hexagonal arrays. Very strong covalent bonds are effective in the layer planes while weak van der Waals forces exist between the layers. High modulus and high strength fibres are achieved when these layer planes are aligned parallel to the fibre axis. The arrangement of the layer planes in the direction perpendicular to the axis of fibres influences their transverse and shear properties [16-17].

However, even after significant progress in the development of C/C composites for aerospace structures, they still have a severe drawback with respect to their poor response to impact loading. The impact induced by rigid masses on composite plates is generally slow, since the time during which the impactor and the plate remain in contact is very long compared with the lowest period of free vibrations of the bodies. Therefore, impact can be treated as a quasi-static

contact because it does not take into account the influence of elastic waves in the interior of the composite plate. Due to localized impact-induced damage, the structural integrity of composite reduces significantly with the creation of matrix cracking, delamination and fibre breakage.

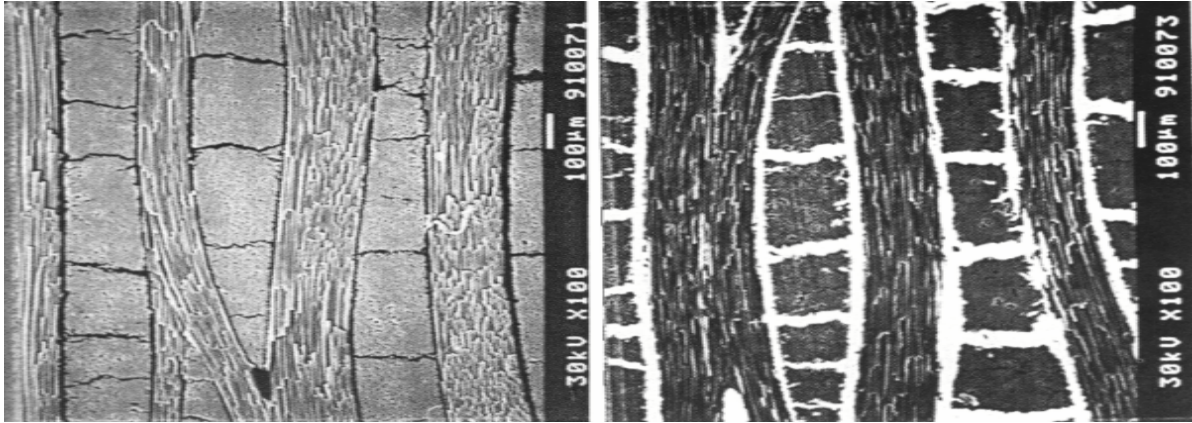


Fig. 2. Left handside micrograph of after pyrolysis at 900°C and right handside after silconising process.

These cracks grow into the interlaminar region between crossed plies, and they can be redirected into the interply as delaminations, if the impact energy is high enough. The delamination caused during the fracture event severely reduces the residual compressive strength of most laminated composites [18]. The presence of delamination may degrade severely the stiffness and strength of composites and in some cases lead to catastrophic failure. Thus, if composite materials are to play a more important role in industry, then a reliable integrity assessment system has to be developed. The principle behind damage detection methods based on model analysis is that damage reduces the dynamic stiffness (EI) of a structure, which results in reduction of the resonant frequencies [19]. The modulus of elasticity (E), velocity of sound (C_s) and density of material (ρ) are correlated [20]:

$$C_s = (E/\rho)^{1/2} \tag{4}$$

Where, sound velocity (C_s) is related to the frequency (f) and wave length (λ) by

$$C_s = f\lambda. \tag{5}$$

Combining equation (4) and (5)

$$f = 1/\lambda(E/\rho)^{1/2} \tag{6}$$

The above equation shows that the resonant frequency is related to the elastic modulus of the material. From the rule of mixture, it is also clear that the elastic modulus of the composite (E) is dependent upon the elastic modulus of fibre (E_f)/matrix (E_m) and the volume fractions of fibre (V_f) and matrix (V_m). This can be written as [17]:

$$E = E_f V_f + E_m V_m, \text{ or } \approx E_f V_f \text{ (since, } E_f > E_m \text{)} \quad (7)$$

$$\text{Therefore, } E \cong V_f. \quad (8)$$

Equation (7) and (8) can be used to explain the influence of the damage on resonant frequency. Thus, the measurement of resonant frequencies of a structure at any stage of its life offers the possibility of detecting the presence of damage. Monitoring the changes in modal frequencies can help assess the structural damage, where the frequencies can be measured accurately as in quality control during manufacture.

The effect of impact damage on the flexural resonant frequency and flexural modulus of C/C–SiC composites is studied in the present investigations. The damage was introduced by the impact caused by dropping a weight from different heights on the specimen. The elastic modulus of the material was determined by grindosonic method, and the crack pattern was monitored by laser confocal scanning microscopy.

1.3. Comparative chart of C/C and C/C-SiC composites [20]

C/C	C/C-SiC	Materials
Schunk, FRG	DLR, FRG	Producer
Polymer Pyrolysis	LSI	Process
1.55-1.65	1.8-1.95	Density, g/cm ³
5-8	2-5	Open Porosity, %
150-200	120-190	Tensile Strength, MPa
70-90	50-70	Young's Modulus, GPa
200-240	200-290	Flexural Strength, MPa
-	210-320	Compressive Strength, MPa
-	55-60	Shear Strength, MPa
8-12	25-30	Interlaminar Shhear Strength, MPa
(RT-1000 ⁰ C)	(RT-1500 ⁰ C)	Coefficient of Thermal Expansion, 10 ⁻⁶ 1/K
0.8	1-2	11 to the fabrics = to the fabrics
6.9	4-6	
60-8	8-29	Thermal Conductivity, W/mK
15-25	6-22	11 to the fabrics = to the fabrics

2. EXPERIMENTAL PROCEDURE:

2.1. Materials Preparation and tests

2.1.1. C/C composites

The material used in this programme was supplied by NFTDC, Hyderabad, India. Small substrates of size 12.5 mm x 12mm x 18mm were cut from laboratory prepared 4D carbon–carbon composite panel having coal tar pitch as matrix precursor with high and uniform fiber content. The average density of the composite was 1.987 g/cm³ with local hardness varying from 542Hv1 (20 seconds) as minimum to 787 Hv1 (20 seconds) as maximum. The frequent hardness values were varying between 728 to 787 Hv1. After being hand-polished using 80 grit SiC paper, these specimens were cleaned ultrasonically with acetone and dried at 373 K for 2 h. The silicon carbide conversion coating was performed at 1873K for 2 hours. It was followed by development of MoSi₂-Al₂O₃ and B₄C coating on these SiC coated C/C substrate through insitu reaction sintering.

The dynamic and isothermal oxidation testing were carried out up to 1473K in thermal analysis system capable of measuring the remained mass in the desired time interval. The system is having an open air circulated furnace of size 120 mm diameters and 200 mm length. The low magnification microstructure of the as prepared C/C composite, coated composite before and after oxidation test were observed using a stereo microscope. The phase contents of samples including tested one were determined using the Philips Xpert pro diffractometer having accelerator detector at 40Kv-30amps power. The thickness of the coating were determined through an optical microscope BX60M of Olympus using ‘image-Pro plus v5.0’ software. Archimedes principle was used to find the density of the samples.

2.1.2. C/C–SiC composite

The investigations refer to cross-woven C/C–SiC composites with HTA carbon fibre ($\phi=7\ \mu\text{m}$) as reinforcement, and the matrix was silicon carbide. The material parameters are shown in Table-1.

Table 1. Material parameters

Parameter	Value
Oreintation	0/90°
Volume fraction, %	
Carbon	60
Silicon Carbide	38
Silicon	2
Density, g/cm³	1.85
Elastic Modulus, GPa	65
Poisson's Ratio	0.182

The material used was manufactured and supplied by DLR (German Aerospace Centre), Stuttgart. First, carbon fibre reinforced plastic (CFRP) composite is prepared using standard industrial process of resin transfer moulding (RTM). The CFRP is then pyrolysed at 900°C in nitrogen atmosphere for the conversion of the resin matrix into carbon. The carbon yield of the precursor is about 60% by weight, which is accompanied by high shrinkage of the resin up to about 20% in length. This results in a high amount of matrix cracking which can be distinguished in irregularly spaced segmentation cracks, micro-delaminations and fibre-matrix debondings within the segments. In the last stage, carbon-carbon is infiltrated with the molten silicon at 1650 °C in vacuum. Silicon infiltrates the C/C preform rapidly and reacts with both fibre and matrix to form silicon carbide. Silicon can enter the material only through segmentation cracks and micro-delaminations during the infiltration process. However, silicon can only infiltrate them partly because some of the cracks are isolated, and at others the crack opening is so small that it is closed by the SiC, in which unreacted silicon (2%) can be found. The excess formation reaction rate of SiC is controlled by the diffusion of silicon atoms through the SiC layer into the carbon fibres [5].

2.2. Effect of Oxidation

2.2.1. Exposure with gas flame on C/C-SiC composites

The 2D C/C-SiC composite plates were cut from the bulk with dimension (1cm x 1cm). The specimens were cleaned ultrasonically to remove any incompact particle and dried. The samples were weighted by electronic balance without any exposure and the surface of C/C-SiC composite was oxidized at temperature about 700⁰C with the gas flame of Oxy-Acetylene torch, which is shown in Fig. (3). The distance was tried to maintain 10mm in between the nozzle of gas and surface (Fig. 4). C/C-SiC composite plates were oxidized with the variation of the time such as 5 min 10 min, 15 min and 20 minutes and they were weighted again. The cumulative weight change of samples was reported as a function of oxidation time, as shown in Fig. 5 and skelton of fibres are visualized from Fig. 6. Percentage of weight loss (ΔW) of the samples were calculated by the following equation

$$\Delta W = [M_0 - M_1] / M_0 \quad (9)$$

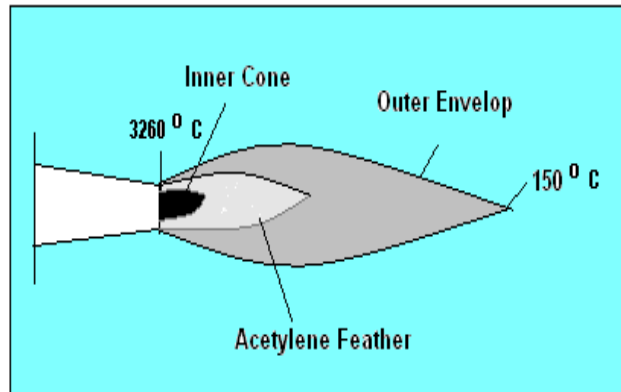


Fig. 3. Profile of oxy-acetylene torch.

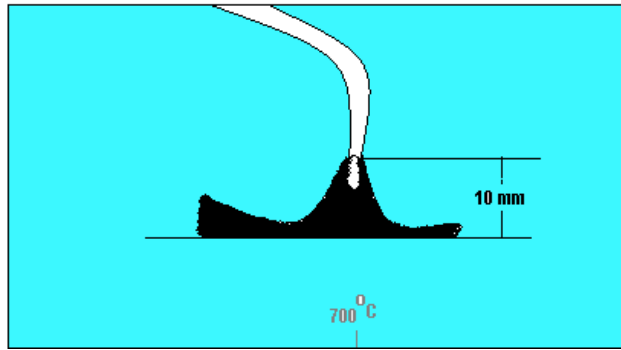


Fig. 4. Flame compressed with surface of C/C-SiC composites.

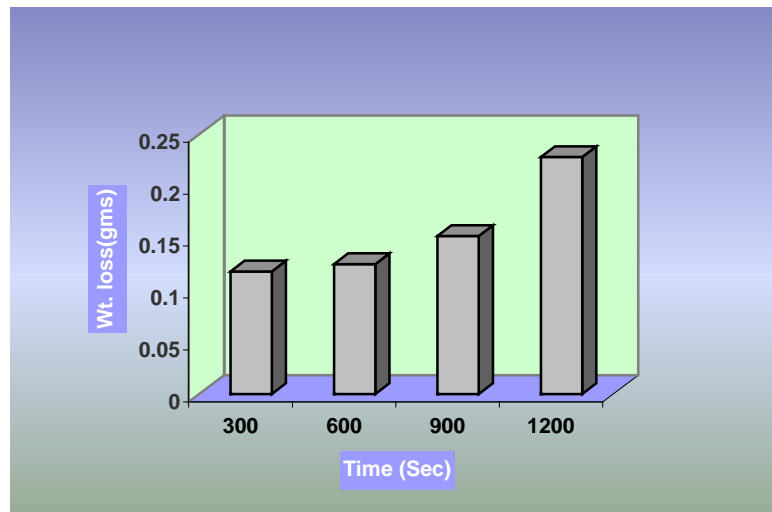


Fig. 5. Variation of weight loss with the variation of time.

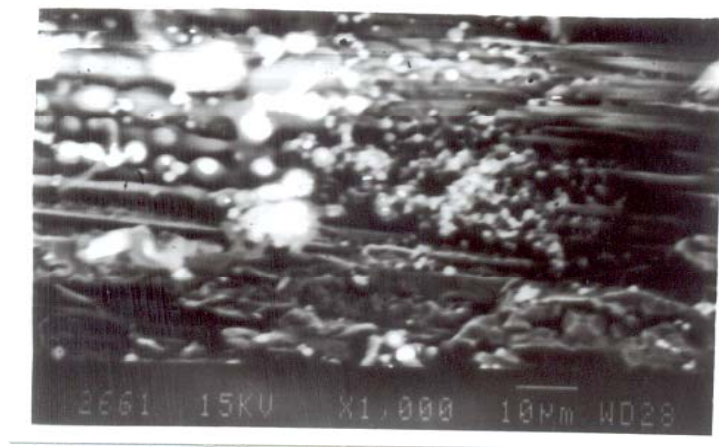
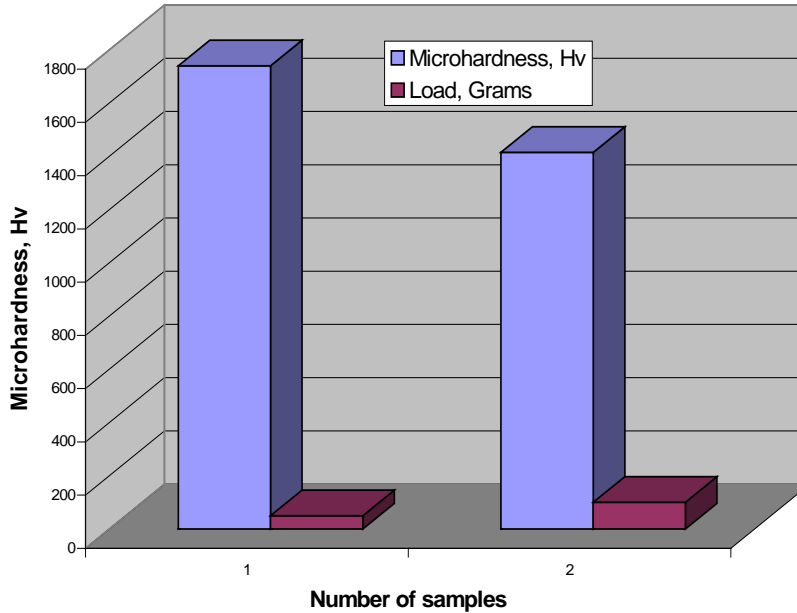


Fig. 6. Skelton of fibres after the exposure of gas flame.

2.2.1.1. Microhardness tests

Fig. 7 . Variation in microhardness with load of unexposed C/C-SiC composites



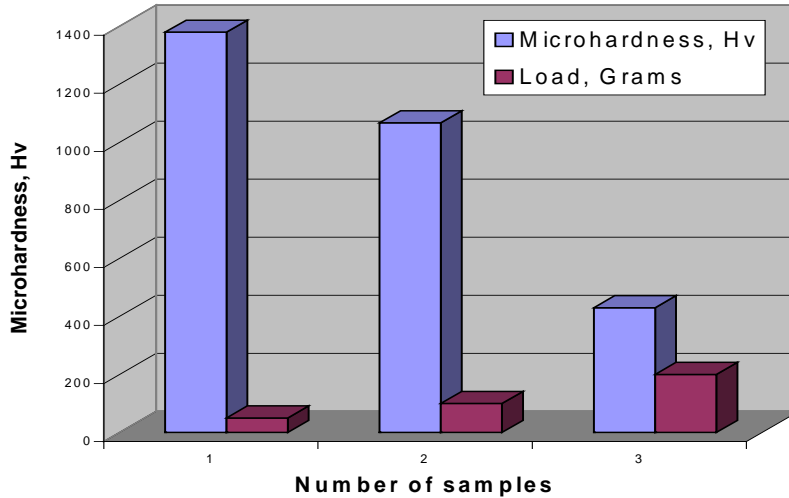
Microhardness test is conducted on Shimadzu microhardness tester (HMV-2T). Indenter is made of diamond in the form of a square based pyramid with an included angle of 136° between opposite faces. The hardness tester is semi-automatic in which the specimen surface is brought close to indenter, the preset load is applied for some definite time and load is removed automatically. The loads are slowly applied to avoid error due to inertia effects. The time of load application and load duration can be controlled. In the present study, the load ranging from 10 to 100 g is applied for the duration of 5 s and Vickers hardness number is calculated using the following equation

$$H_v = 0.1891 \frac{P}{d^2} \text{ and} \quad (10)$$

$$d = \left(\frac{H + V}{2} \right) \quad (11)$$

where P is the applied load (N), d is the diagonal of square impression (mm), H is the horizontal length (mm) and V is the vertical length (mm). Variation of microhardness in various samples before and after oxidations is plotted in Figs. 7 & 8.

Fig. 6. Variation in microhardness with load of exposed C-C/Sic composite



2.2.1.2. XRD and Thermal analysis

The oxidized and unoxidized samples were passed through the XRD analysis to find out the change in mechanical behavior of oxidized and unoxidized samples are mentioned in Fig. 9 & 10. The morphology of each specimen was quite different on microscopic scale due to conditioning of specimen and loads.

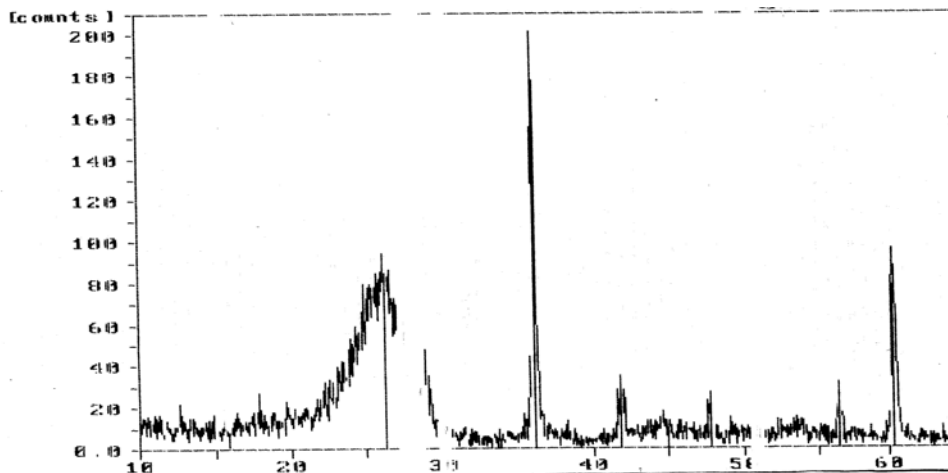


Fig. 9. XRD patterns of unexposed C/C-SiC composites

Also, unoxidized and oxidized samples were treated with Perkin-Elmer thermal analysis to study the behavior of samples toward the temperature are illustrated in Figs. 11 & 12..

Finally, scanning electron microscope test was used to evaluate the morphology of fractured samples.

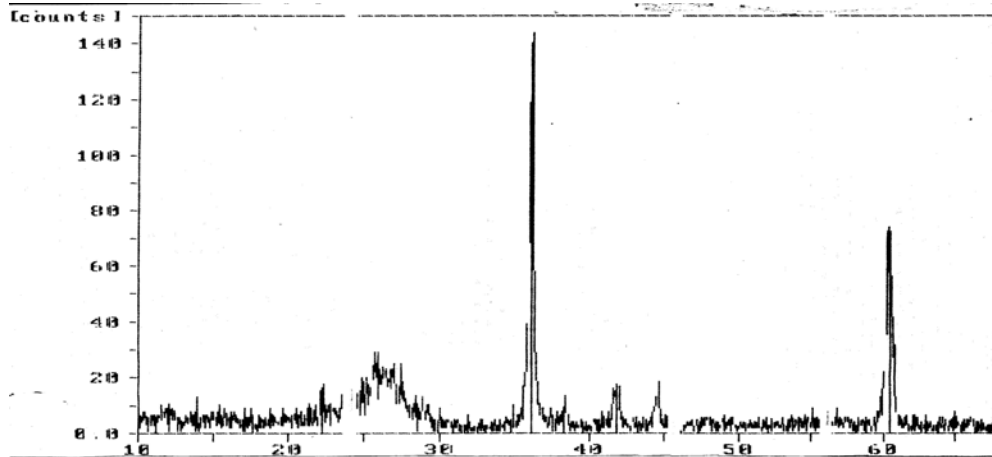


Fig. 10. XRD pattern of exposed C/C-SiC composites.

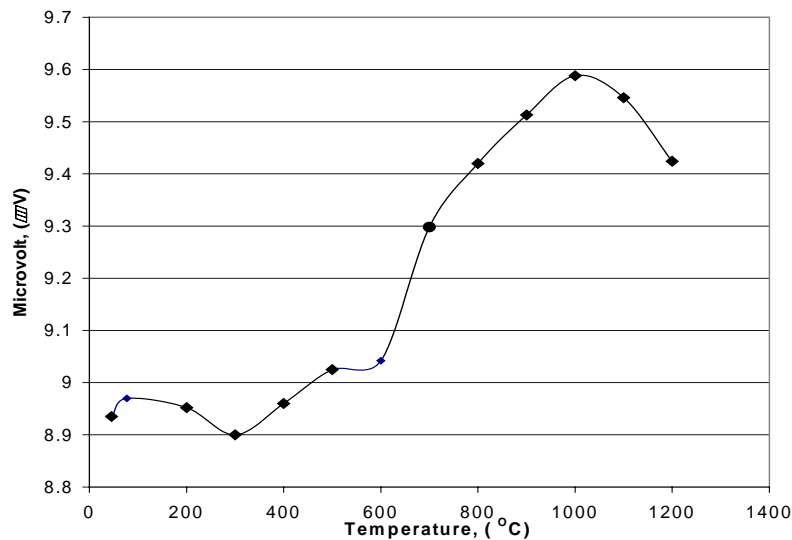


Fig. 11. Variation of microvolt with temperature of unexposed C/C-SiC composite

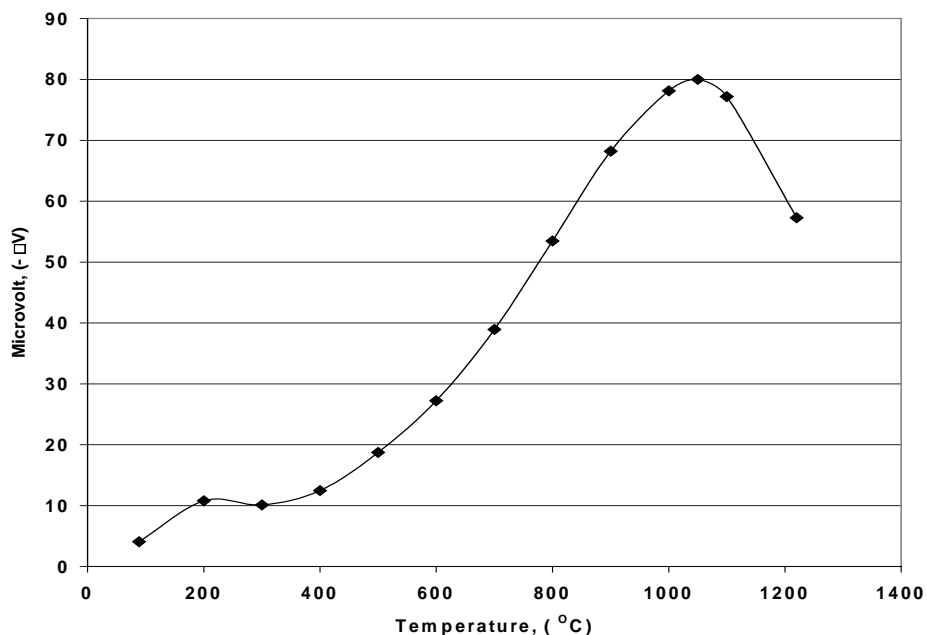


Fig. 12. Variation of microvolt with temperature of exposed C/C-SiC composites

2.2.2. Exposure of temperature on 2D and 4D C/C Composites

Fig. 13 predicts the loss of dimensions as well as 54 % weight loss of a square shaped graphite of density 2.1g/cm^3 exposed up to 1473K for 20 minutes in dynamic heating and 120minutes as isothermal heating condition. The non symmetric and conical appearance of the graphite as seen in the Fig. 13, predicts the uneven surface profile created due to existence of a turbulent air flow in the thermal analysis system. The microstructure of the 4D composite has been shown in Figs. 14 and 15. The line type and circle type appearance are the fiber bundles having the carbon matrix in between them. The phases as detected from powders were obtained by uniform sawing of the composite along the transverse direction. The detected phases were 5% of hexagonal graphite having unit cell volume as 22.25A^3 , 51 % of hexagonal graphite having unit cell volume as 35.5A^3 , 39% of hexagonal graphite having unit cell volume as 52.45A^3 , 5% of cubic carbon having unit cell volume as 79.12A^3 and very small amount of non-quantified

rhombohedral C70 with 2251.86 \AA^3 . The finely distributed ‘crater appearance’ as observed in the figures are the pores developed during the fabrication of the composite.



Fig. 13. Loss of shape and weight (54 w%) of a square shaped dense carbon composite expose up to 1473K for 140 minutes.

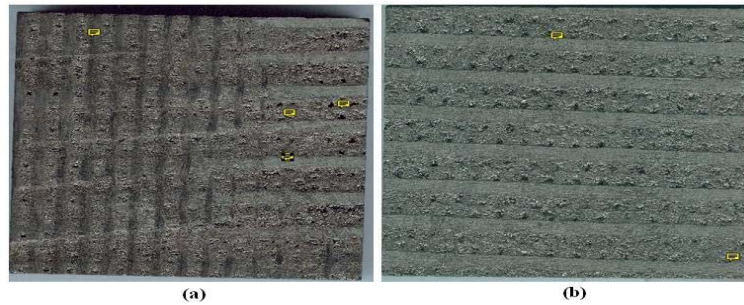


Fig. 14. Longitudinal views of microstructure of 4D bare carbon composite at 8x

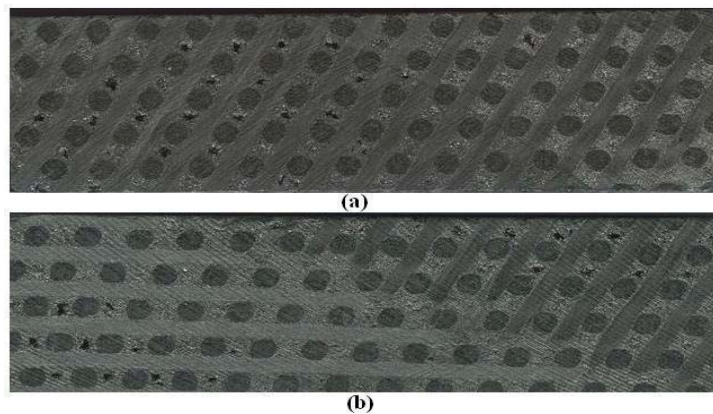


Fig. 15 . Transverse views of microstructure of 4D bare carbon composite at 8x

As seen in Figs. 16 and 17, the loss of weight of uncoated 4D composite was 30 w% with 60 minutes isothermal exposure at 1273K. The diminishing shape of the composite was occurred along the surface following the hot air turbulence as discussed for the dense graphite. The intra oxidation was not significant. The figures show the initiation of the internal oxidation between the carbon fiber bundle and the interface with matrix were preferably attacked creating a rough surface.

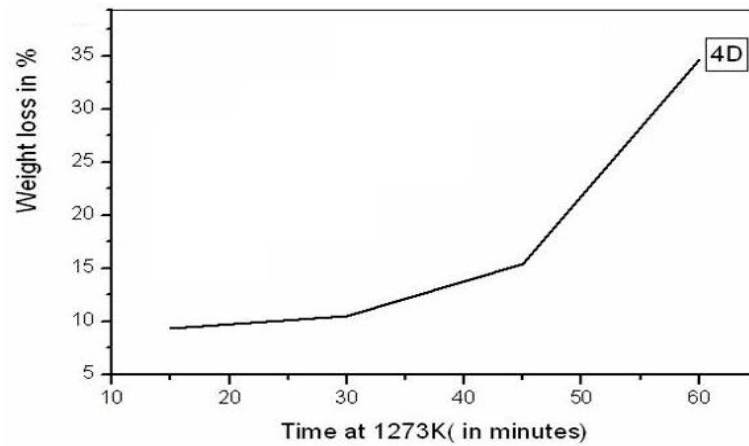


Fig. 16. Loss of weight in % of 4D bare composites at 1273K for (15,30,45,60) minutes

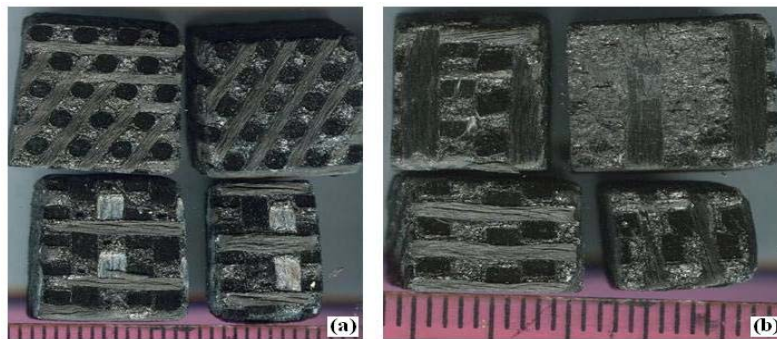


Fig. 17. Loss of shape of 4D bare composites at (15, 30, 45, 60) minutes (anticlockwise).Figure shown in 8x

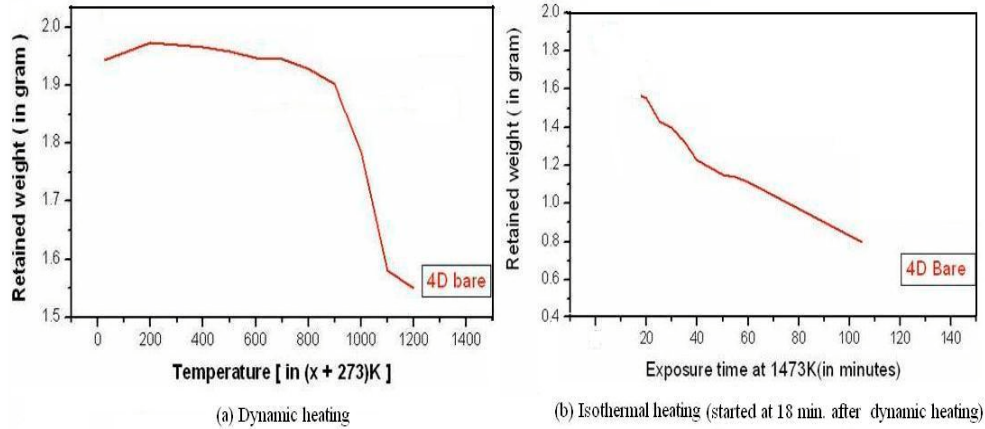


Fig. 18. Weight of 4D bare as retained in dynamic and isothermal heating condition.

The 4D composite in as-fabricated condition exhibited four type of oxidation regime as in Fig. 18 (a and b). The initial linearity up to 948K indicated the slow surface reaction between the carbon and oxygen molecules. The change in linearity in-between 948K-1100K shows the intermediate region where oxidation increased by gaseous diffusion. There was a sharp increase in surface reaction at crater type defect sites and gaseous diffusion in-between 1100K and 1373K. After 1373K the inward diffusion of oxygen slowed down due to incoming CO and CO₂ gases. However the built up pressure inside the composite started cracking it and thus with isothermal hold at 1473K, the fall in weight of the composite was comparatively faster. After a total of 100 minutes dynamic as well as isothermal heating, the whole block of the composite kept for testing collapsed. In all cases it was observed that matrix carbon started oxidizing faster compared to fiber carbon.

2.2.2.1. Oxidation performance of SiC coatings on C/C composites:

The density and thickness of coatings as determined for coated samples have been presented in Table 2.

Coating type on C/C	Thickness (in micron)	Density (g/c ³)
SiC	460	2.06

Table 2. Density and thickness of coatings SiC on C/C

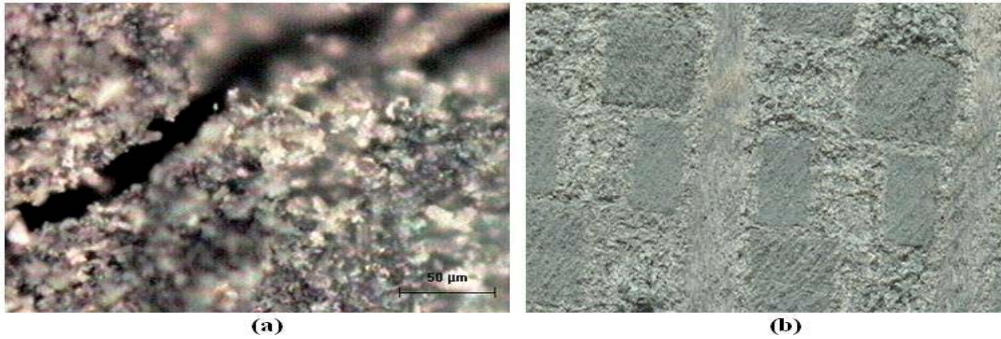


Fig. 19. (a) A 20 μ x 250 μ sized cracked as seen in one portion of the SiC coated on C/C and (b) Macrostructure of the SiC coating on C/C at x 8.

As observed in Fig. 19, rough grayish green region were the matrix region having a crack (Fig 19-a). Rough dark grey region were the matrix region with white spotted alumina regions. However matrix region although got coated still was rough. Two type of hexagonal SiC (49w %) and three type of SiO₂ (tetragonal: hexagonal: orthorhombic with w% as 5:14:32) were detected in the oxidized product. Nearly 41w% of SiC has been oxidized to SiO₂. However matrix region although got coated still was rough. cubic (17w %) and hexagonal (66w %) SiC, cubic (7w %) Si₃C₃ and 10w% graphite were detected in the as coated SiC – C/C composite (Fig. 20). It showed cubic SiC is relatively less stable compared to hexagonal SiC. The oxidation weight loss was 34.7%.

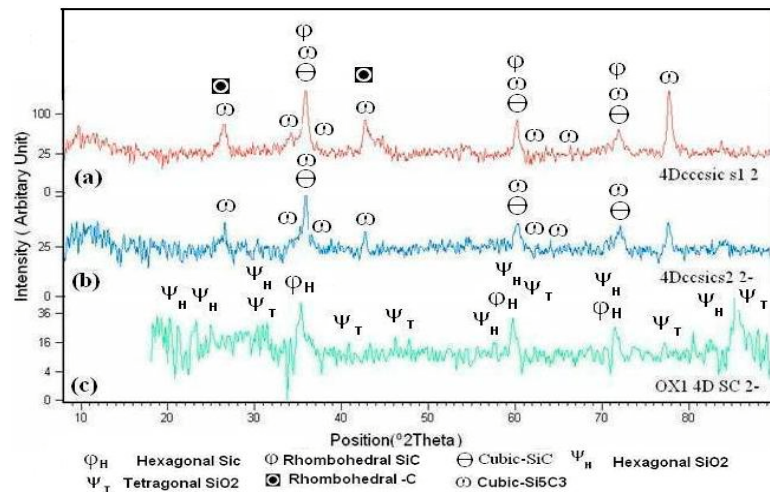


Fig. 20. X-ray diffraction of SiC coating on 4D C/C (a) before oxidation (portion1), (b) before oxidation (portion 2) and (c) after oxidation

2.2.3. Mechanical performance

2.2.3.1. Tensile and compressive tests

The tension and compression tests were generally performed on flat specimens. The most commonly used specimen geometries are the dog-bone specimen and straight-sided specimen with end tabs. A uniaxial load is applied through the ends. The ASTM standard test method for tensile properties of fibre–resin composites has the designation D3039-76. It recommends that the specimens with fibres parallel to the loading direction should be 12.7 mm wide and made with 6–8 plies. Length of the test section should be 153 mm. The test-piece used here is of dog-bone type and having dimensions according to the standards. The tensile and compressive tests were performed on the universal testing machine (Fig. 21) and results were analyzed to calculate the tensile strength of composite samples.

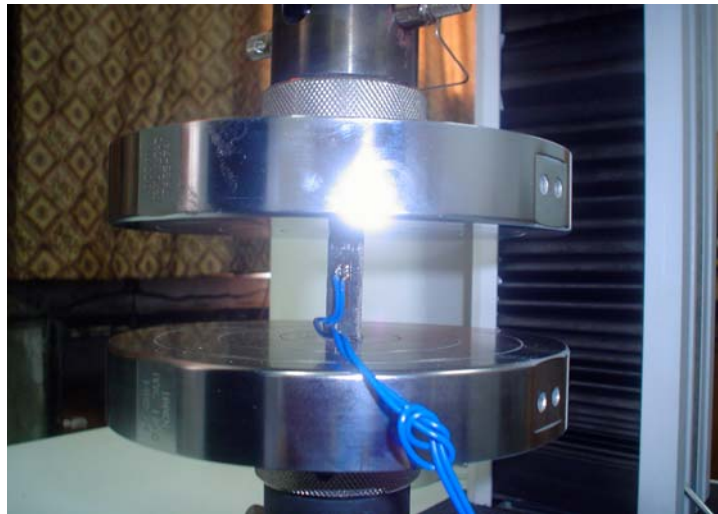


Fig. 21. Experimental set-up of mechanical test.

Compression test:

First of all, compression test was performed on the exposed and unexposed samples of C/C-SiC and C/C composites. The rectangular sample was fixed in the UTS machine and compressive load was increased. The sample was crushed out from the lower edge, as shown in Fig. 22 & 23.

C/C-SiC composite was fractured abruptly with the combined effects of fibre bending, matrix cracking, debonding and delamination.

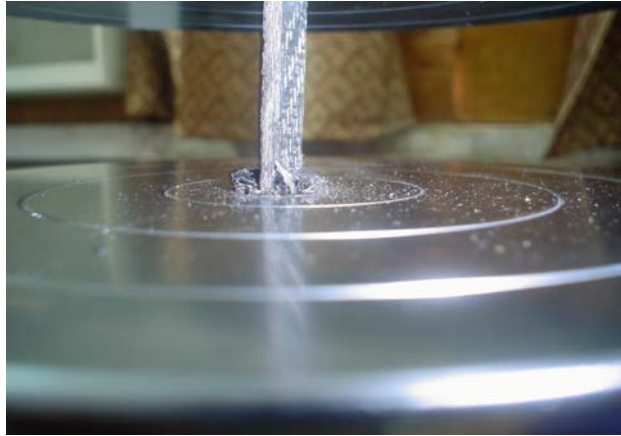


Fig. 22. Fracture deformation of C/C-SiC under compression



Fig. 23. Damage sample of oxidized C/C-SiC under compression

Maximum stress was recorded for each sample and results were plotted against the exposure time to see the loss of strength as can be illustrated in Fig. 24 & 25.

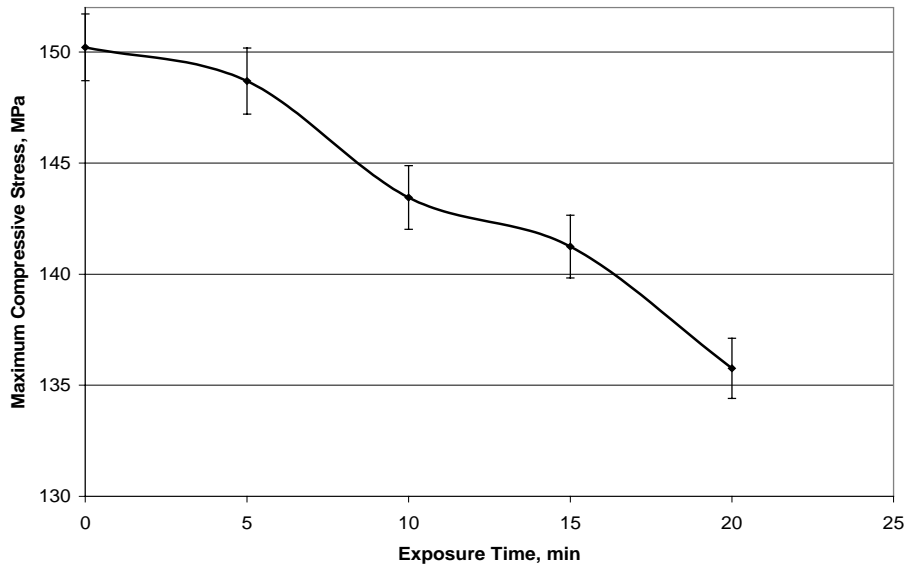


Fig. 24. Degradation of maximum compressive stress with increase of exposure time of gas flame on C/C-SiC

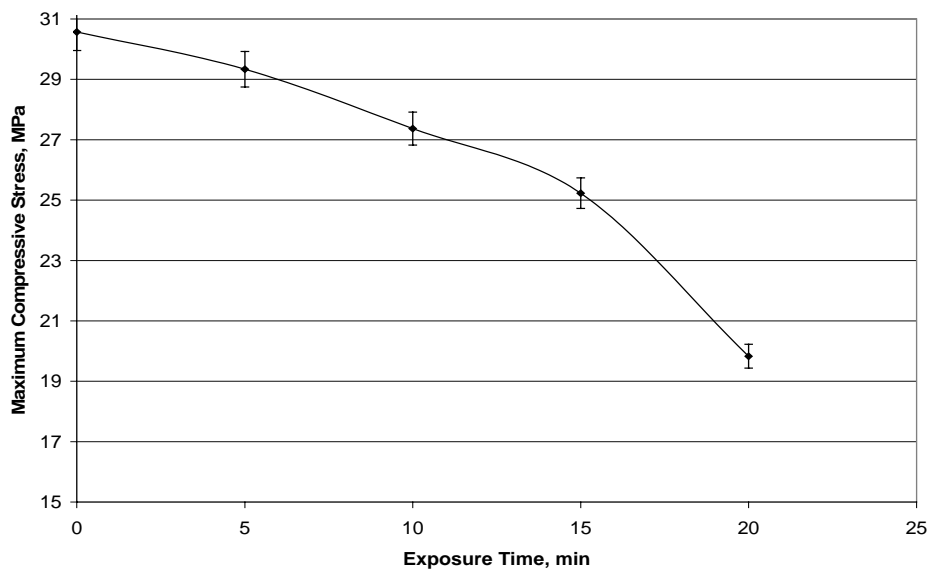


Fig. 25. Degradation of compressive stress with increase of exposure time of gas flame on C/C

Tensile test:

All composite samples were exposed to the flame of oxyacetylene gas in an open atmosphere with a variation in time from 5 min to 20 min. The exposed samples are shown in Fig. 26. Each sample was fixed in a UTS machine to determine the maximum tensile stress. The load versus displacement curve was plotted for C/C-SiC and C/C composites, as shown in Fig. 27. The maximum stress of each sample was also recorded to observe the change in strength with increasing exposure time, which is shown in Fig. 28 and 29.

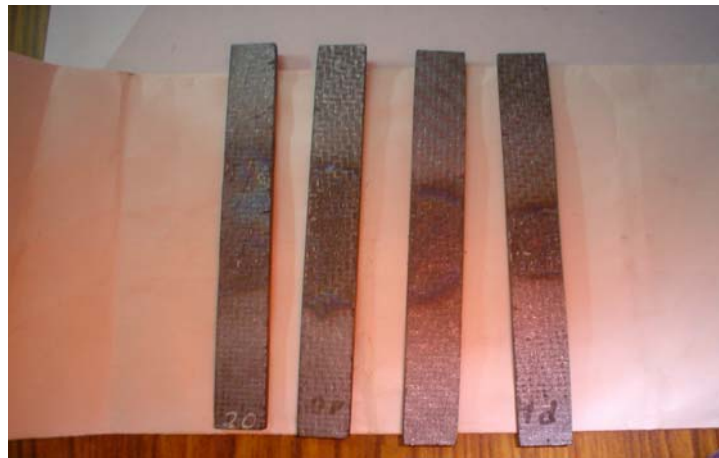


Fig. 26. Exposed C/C-SiC samples with oxyacetylene gas flame

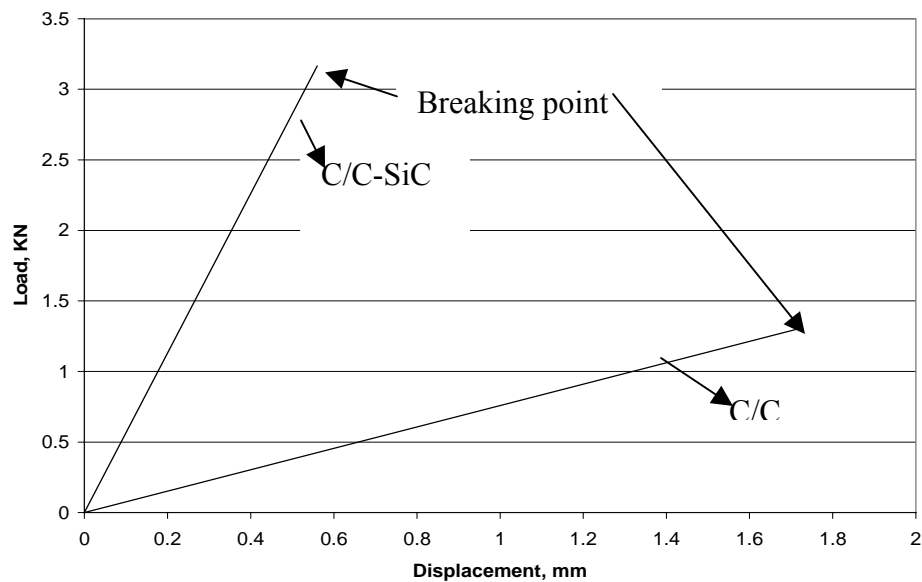


Fig. 27. Variation of load with displacement of oxidized composites under tension.

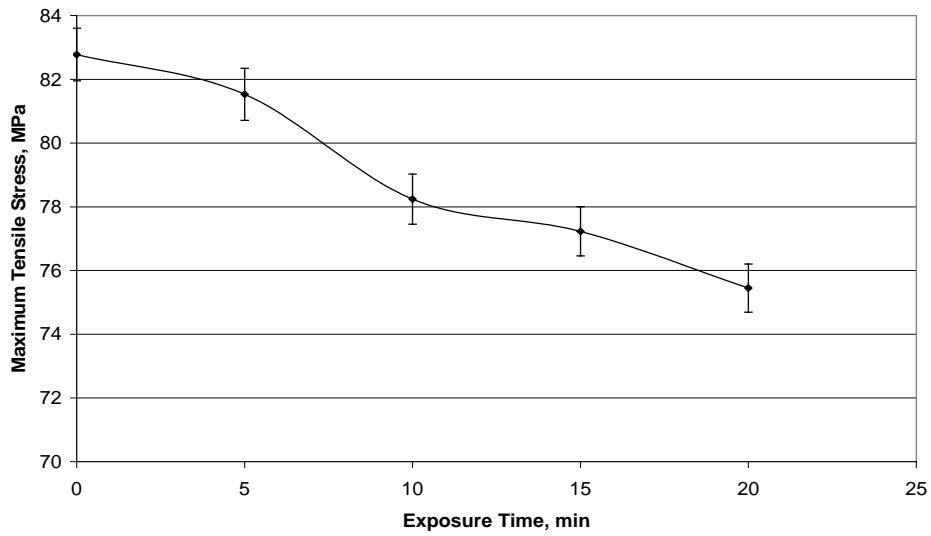


Fig. 28. Degradation of tensile stress with increase of exposure time of gas flame on C/C-SiC

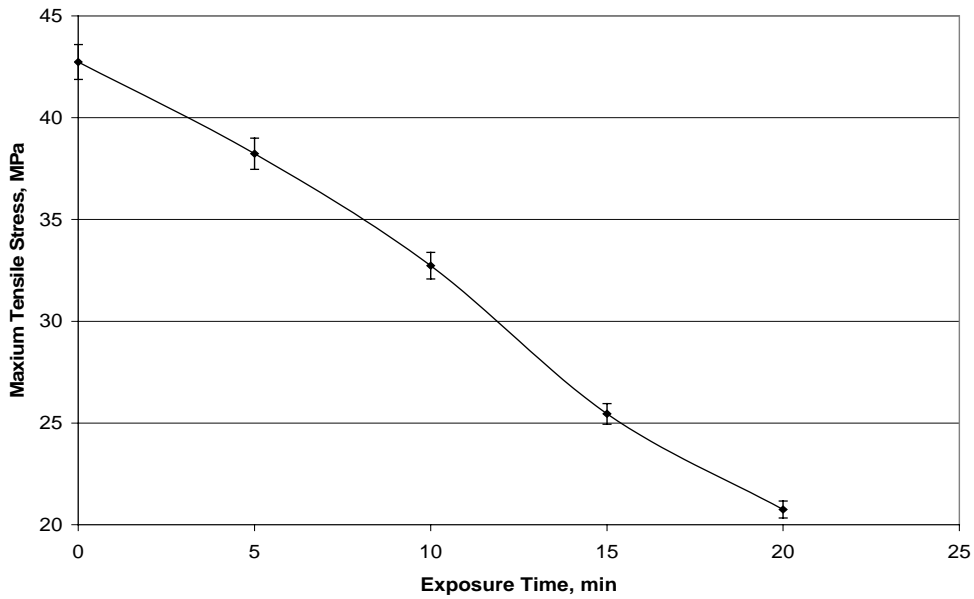


Fig. 29. Degradation of maximum tensile stress with increase of exposure time of gas flame on C/C composite

2.2.3.2. Scanning electron microscopy test:

The fractured surface of oxidized and unoxidised C/C/SiC and C/C composite specimens was observed by scanning electron microscope (SEM) method. The deformation of fibres, matrix and distribution of Si, SiC were quite different on microscopic scale due to conditioning of specimen and load, which images are shown in Figs. 30-33.

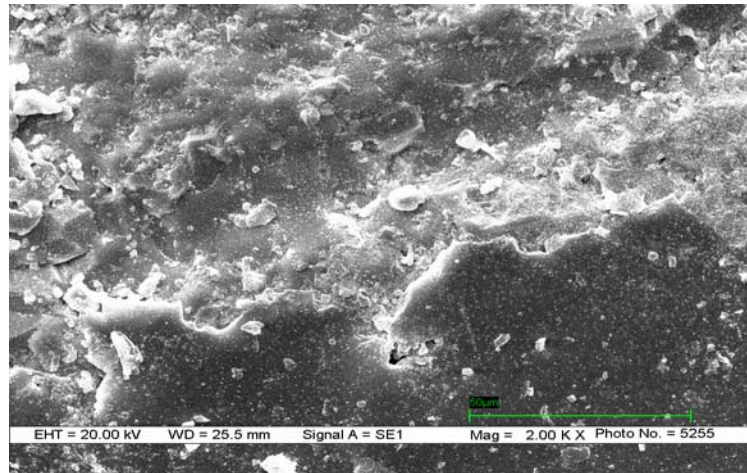


Fig. 30. SEM of C/C/SiC composites without fracture

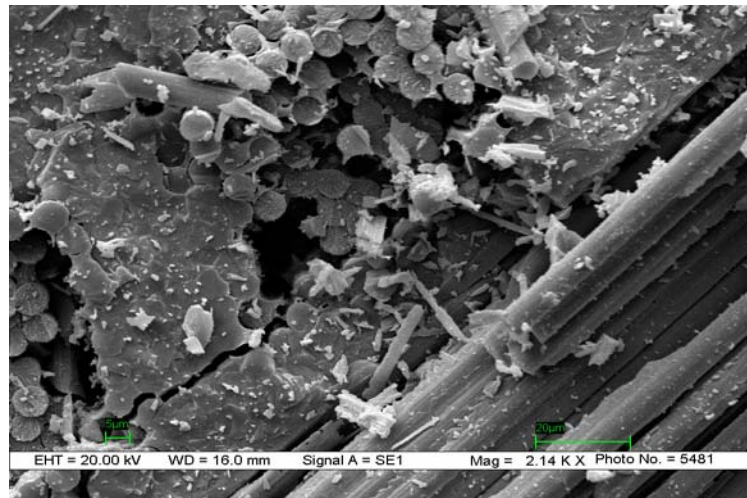


Fig. 31. SEM of fractured sample of C/C-SiC composites.

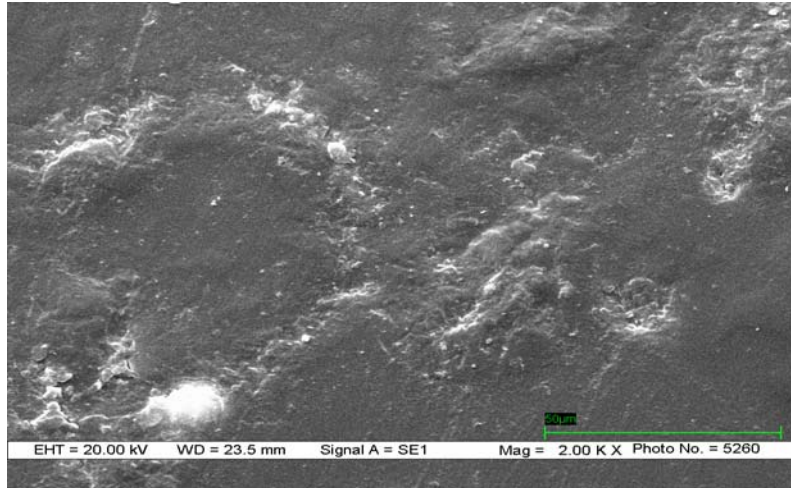


Fig. 32. C/C Composites without fracture.

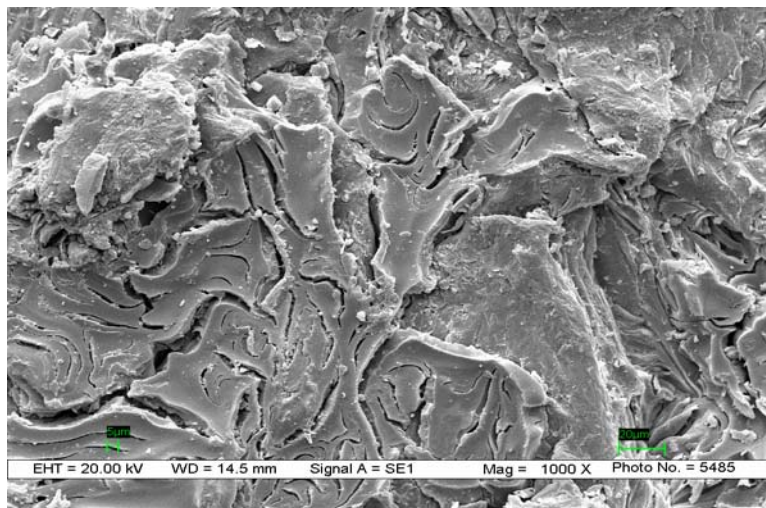


Fig. 33. Fractured sample of C/C composites.

3. DISCUSSIONS:

3.1. Effect of oxidation on composites

Due to oxidation of carbon in open atmosphere, C/C-SiC and C/C composites properties was decreased with increase of exposure time. In the process of oxidation, the matrix undergoes pyrolysis reaction within short period of time. This generates volatiles and leaves behind a

porous skeleton of carbon fibres on outer layers and reduces weight of virgin C/C-SiC (2%) and C/C (>12%) composites. The overall effects on tensile and compressive stress of the composites can be clearly visualized from the Figs. 24, 25, 28 & 29. The degradation in maximum tensile stress and compressive stress of C/C-SiC was obtained 8.82% during oxidation process, whereas, maximum tensile stress and compressive stress of C/C composite was reduced more than 29.32%. This shows that the C/C composite was easily oxidized in open atmosphere. It's clearly indicated that the composite surface texture is fully oxidized with the oxidation effect, which creates more microcracks due to degradation carbon and matrix / fibre interface, as can be seen from Fig. 32 & 33. However, thermal expansion coefficient of SiC ceramic is largely higher than that of C/C composite, which induced the formation of cracks. The cracking is caused by stress development due to the coefficient of expansion mismatch between the carbon fibres and the SiC matrix. Which also results in through the wall porosity in the composite?

In unexposed sample the average microhardness is 1740.33 Hv under the 50 gm and with 100 gm it was 1415 Hv (Fig.7), whereas in exposed sample it becomes reduced. The value of microhardness is decreased from 1740.33 Hv to 1379.33 Hv under the load of 50 gm, 1067 Hv with 100 gm and 430 Hv with 200 gm (Fig. 8).

This information indicates that the fracture surface of oxidized specimens is different than the unoxidized C/C-SiC composites.

XRD is used for the phase analysis. In the microstructure of C/C-SiC composite, XRD confirms the formation of SiC phase, which are made out of Si vapour exposed with carbon fibres. The microstructure indicates severe reaction between carbon fibre and molten silicon. In the present study, the XRD pattern used for both type of samples oxidized as well as unoxidized (Fig. 9) shows the microstructure of unexposed C/C-SiC composite and in Fig. 10, which tells about exposed C/C-SiC the number and height of peaks become reduced.

This reduction in number and height of peaks is due to the morphological change in the sample. After oxidation carbon degraded in the form of carbon-di-oxide and carbon-mono-oxide ($C+O_2 \rightarrow CO_2\uparrow$, $2C+O_2 \rightarrow 2CO\uparrow$) and Si reduce in the form of silicon oxide ($Si+O_2 \rightarrow SiO_2$).

Due to the loss of carbon and silicon particle from the sample, the morphological characters were changed and hence the reduction in number and height of peak obtained.

Thermal conductivity is a key property in many applications of C/C-SiC composites. Generally these are relatively good conductors of heat but their conductivity depends upon the crystallinity

of their constituents. And due to change in the proportion of oxygen, carbon and silicon, the conductivity becomes also changed. Figs. 11 and 12 shows the thermal behavior of unoxidized and oxidised C/C-SiC composites, which clearly indicates that the microvolt increases with increased of temperature. Whereas the value of microvolt unoxidized is reduced 2% from oxidized samples. However the value of microvolt increases with increase of temperature upto 1000°C and then reduced abruptly with increase of temperature. The change in texture of oxidised composite shows different behavior from unoxidized sample as can be identified from Fig. 13.

Micro cracking of the matrix increased in weight loss. The cracking was due to the residual stress field formation resulting from the thermal expansion anisotropy developed because of presence of Si and Si-C phases. However the coating was too hard before and even after oxidation. On a gentle loading a portion of coating was removed showing the enhanced brittleness of the coating after exposed to high temperature.

The surfaces of the oxidation tested samples were identical to the surface before testing. The most remarkable point was that the matrix was fully protected from oxidation while localized oxygen attack was observed on the fiber bundles (Fig. 17). Almost all sets of fiber bundle have been oxidized. This could be the wettability difference between the graphitized carbon fiber and the generated phase such as SiO₂. The formation of each phase can be identified from XRD patterns as shown in Fig. 20. Another possibility is of consumption of oxidation protection at these points.

3.2. Micro performance of composites

The micro observation of oxydised and unoxidised fracture sample of composites were illustrated that the virgin composites severally affected by the oxidation in open atmosphere. The variation in maximum tensile and compressive stresses shows that the 2D C/C composite get reduced more than the C/C-SiC composite. Figs. 24, 25, 28 & 29 show the maximum compressive stress of C/C-SiC and C/C composites reduced with increase of exposure time in general. The increased in weight loss caused by microcracks, pyrolysis of matrix and fibre debonding / delamination results in the reduction of strength. The microcracks increased with increase of oxidation of carbon caused by the exposure of temperature in open atmosphere. Figs.

30-33 micrographs are obtained from the fractured samples of oxidized and unoxidised C/C-SiC and C/C composites. As expected with orthotropic materials, the fracture surfaces are perpendicular to the applied load. The detailed investigation revealed that the fracture surfaces are discontinuous; following the network of bundle of fibres is involved in the damaging process. In the first instant, fibres debonded and broken/pulled out with the increase of tensile load, as can be seen from Fig. 31. However, 2D C/C composite fractured just like ceramic tiles with large cracks as can be observed in Fig. 33. Therefore, the results clearly indicate that the maximum tensile and compressive stress decreased with increase of exposure time.

4. CONCLUSIONS:

Based on the experimental observation, the results clearly indicate that weight of C/C-SiC composite is damaged severally at about 2% and 2D C/C composite damaged nearly 12%, when oxidised in open atmosphere by the flame of oxy-acetylene gas. The changes in microhardness, XRD pattern and thermal properties are appeared because of delamination, debonding, pyrolysis of matrix and formation of CO, CO₂ and SiO₂. Therefore, maximum tensile and compressive stress of ceramic composites decreased with the oxidation time in open atmosphere by oxyacetylene gas flame.

Also, SiC ceramic coating on 4D carbon composites resulted that the carbon-carbon composite temperature predicts the oxidation kinetic is severe after 1273K. This was due to formation of smooth silicon carbide film phases covering the surface of the composite. Which is less volatile and showed lower oxygen permeability, and consequently acted as an effective oxygen diffusion barrier? The whole study show that a combination of both silicon and carbon based materials system is more useful for elevated oxidation protection of carbon-carbon composites.

5. REFERENCES:

1. Krnel K., Stadler Z. and Kosmac T. *J., Eur. Ceram. Soc.* 27 (2007) 1211–1216.
2. Inghels E., Lamon, J., *J. of Materials Science*, 26 (1991) 5411-5419.
3. Gac F.D. and Petrovic J.J. *J., Am. Ceram. Soc.* 68-8 (1985) C200–C201.
4. Jeng Y.L. and Laverina E.J. *J., Mater. Sci.* 29 (1994)2557–2571.
5. Gang F.Q., Jun L.H., Hong S.X., Zhi L.K., Min H. and Dong S.G., *Surface and Coatings Technology*, 201-6(2006)3082-3086.
6. Fan Z., Song Y., Li J., Liu L., Song J., Chen J., Zhai G. and Shi J., *Carbon* 41-3(2003)429-436.
7. Kobayashi K, Miyazaki K, Ogawa I, Hagio T, Yoshida H, *Materials & Design* 9-1 (1988)10-21.
8. Piquero T., Vincent T., Vincent C. and Bouix J., *Carbon* 33-4(1995)455-467.
9. Paul F. B. *Journal of the American Ceramic Society*, 66- 8 (1983)C-120.
10. Taylor, R., *Comprehensive composite materials*, Elsevier science Ltd., Boston, (2000) 387-426.
11. Fitzer, E., Manocha, L.M., *Carbon reinforcement and C/C composites*, Springer-verlag, Berlin, (1998).
12. Buckley, J.D., Edie, D.D., *C-C materials and composites*, Noyes publications, New Jersey, (1993), 1-12.
13. Westwood, M.E., Webster, J.D., Day, R.J., Hayes F.H., Taylor, R., *J. Mater Sci.* 31(1996), 1389.
14. Heimann, D., Bill, J., Aldinger, F., Schanz, P., Gern, F.H., Krenkel, W., Kochendorfer, R., *Development of oxidation product Carbon/Carbon.*, *Z Flugwiss Weltraum* (1995); 19: 180-8.
15. Williams, J.C., Yurgartis, S.W., Moosbrugger, J.C., *Interlaminar Shear fatigue damage evaluation of 2D Carbon-Carbon composites*, *J Compos Mater* (1996); 30(7): 785-800.
16. Arendts, F.J., Theuer, A., Maile, K., Kuhnle, J., Neuer, G., Brandt, R., *Thermomechanical and Thermophysical properties of liquid Siliconized C/C-SiC*, *Z. Flugwiss Weltraum*, 1995; 19:189-96.

17. J Schulte-fischedick, J., Zern, A., Mayer, J., Ruhle, M., Frie, B.M., Krenkel, W., Kochenderfer, R., The morphology of SiC in C/C-SiC composites, Mater Sci Eng-A (2002); 332: 146-52.
18. Roos, E., Maile, K., Lyutovich, A., Cusko, A., Udoh, A., (Cr-A) bilayer coating obtained by ion assisted EB PVD on C/C-SiC composites and Ni based alloys, Surf Coat Technol, (2002); 151-152; 429-33.
19. Srivastava, V.K., Maile, K., Klenk, A., High Velocity impact perforation on C/C-SiC composites. High temperature-High pressure, (1999); 31: 487-97.
20. Arendts, F.J., Maile, K., Thermomechanisches Verhalten Von C/C-SiC. Arbeits-und Ergebnisbericht SFB (1998):259.

6. PUBLICATIONS:

- i. V.K. Srivastava and S. Singh, Effect of gas flame on performance of C/C-SiC composites, HTCMC-6, India Habitat Center, New Delhi, Sept. 2007 (Accepted).
- ii. V. K. Srivastava, Oxidation behavior of ceramic composites in open atmosphere, 32nd Int. Conf. & Exposition on Advanced Ceramic & Composites, Hilton Daytona Beach Resort Ocean Center, Jan 27-Feb 1, 2008 (Submitted)

7. WORK SCHEDULE FOR 2nd YEAR:

Following work will be organized to get another set of the results during the second year.

*Ceramic composite will be exposed with the hot water, acid and hydrogen. Mechanical properties of exposed composites will be obtained to describe the effect of above environments.

*Mechanical Characterization of lap joint of C/C-SiC and Ti alloy In this direction, we will firstly prepare the 6 samples of titanium and 6 samples of C/C-SiC of (60×13×3) mm. The surface of samples is first washed with washing powder to remove any foreign material, after some time it will become dry. And again clean with acetone. We will prepare six pair of samples of different type. In three samples araldite and hardener used as an adhesive in the ratio of 1:10 and in another three samples we will also add Si powder in araldite epoxy adhesive. In first piece, the C/C-SiC and Ti sheet were joined; in second piece Ti and Ti were joined and in third piece C/C-SiC and C/C-SiC were joined in the fashion of single lap joint. From these we will study the mechanical characterization of different type of samples. We will study the property and strength of joints under SEM and TEM.

* Simulation study will be carried out with the help of various computer programming. Finally the analytical and experimental results will be correlated with each to find the variation in results.

8. Grant required for second year:

Grant require for the completion of proposed research work is \$ **23160**.